Confinement of fast ions and FLR effects in presence of magnetic islands

Julio J. Martinell and Leopoldo Carbajal

Instituto de Ciencias Nucleares, UNAM, A. Postal 70-543, México D.F., Mexico

I. Introduction. Fast ions are very important in many aspects of toroidal devices for plasma confinement. They appear mainly in relation to plasma heating from auxiliary sources such as NBI and ICRH where the injected energy is concentrated in a small population of energetic particles which have to transfer their energy to thermal particles by collisions. Fast ions have to be well confined before thermalizing in order to optimize heating. However, the presence of magnetic perturbations such as magnetic islands may increase the transport and reduce the confinement time which would reduce heating efficiency. On the other hand, for moving perturbations, such as rotating magnetic islands, the associated poloidal flow may reduce the transport. To explore these effects we study the transport of fast ions that cross the region of magnetic islands under different circumstances. Islands can be formed spontaneously by neoclassical tearing modes (NTM) or created from the outside by resonant magnetic perturbations.

Neoclassical transport has been developed for toroidal plasmas nested magnetic surfaces and in order to include the effect of magnetic islands present at low-order rational magnetic surfaces a Monte Carlo simulation is used by means of both guiding center (GC) [1] and full orbit (FO) [2] codes. We do not take into account the excitation of MHD modes which in turn may change the background magnetic fields. A similar study was carried out for runaway electrons comparing guiding center (GC) with full orbit (FO) computations [3]. Here we focus on finite Larmor radius (FLR) effects on fast ion radial transport, particularly when it is of the order of the island width. The codes are validated by computing the transport coefficients and comparing with neoclassical theory. We consider a population of fast ions inside the radius of the rational surface that contains the islands and measure the flux of crossing particles as they thermalize via collisions with a Maxwellian plasma background, which are described by Lorentz scattering [4]. The initial particle distribution is monoenergetic and has a single pitch angle. The presence of island rotation as well as the inclusion of an electric field associated with the NTMs are also included in the study.

II. Model for the tokamak magnetic field with islands. The equilibrium magnetic field is modeled by nested circular toroidal flux surfaces which in toroidal coordinates is given by $\mathbf{B}(\mathbf{r},\theta) = \left[\mathbf{B}_\zeta(\mathbf{r},\theta)\hat{\mathbf{e}}_\zeta + \mathbf{B}_\theta(\mathbf{r},\theta)\hat{\mathbf{e}}_\theta\right]$ where

$$B_\zeta(r,\theta) = Bo/(1+\varepsilon\cos\theta), \quad B_\theta(r) = \kappa\varepsilon B_0/[q(r)(1+\varepsilon\cos\theta)]. \tag{1}$$

with $\varepsilon = r/R_0$, $\kappa = \hat{\mathbf{B}}_\zeta \cdot \hat{\mathbf{J}}_\zeta$ and $q(r) = q_0\left(1 + \frac{r^2}{\varepsilon^2}\right)$. The magnetic island filed is given through a perturbation $\delta B = \nabla \times \delta A$ where $\delta A = \tilde{\alpha}(r,\theta,\zeta)R_0\mathbf{B}(\mathbf{r},\theta)$, $\tilde{\alpha}(r,\theta,\zeta) = \alpha(r)\cos\varphi_{mn}$, with $\varphi_{mn} = n\zeta - \kappa m\theta + \omega_{m,n}t$, $\alpha(r) = \alpha^*(r/r^*)[(a-r)/(a-r^*)]^p$. The associated island width is $\delta r_{mn} \approx \sqrt{\frac{4q(r)b(r)R_0}{nq'(r)}}$ where $b(r) = m\alpha(r)R_0/r$.

The field magnitude is $B(r,\theta)/B_0 = 1 - \varepsilon\cos\theta$. This is the only function required in the GC code. Values of a DIII-D-like tokamak are used with $B_0 = 2$ T, $R_0 = 1.5$ m, $a = 0.5$ m, $q_0 = 1$, $q_a = 5(\varepsilon = a/2)$, and plasma current $I_p \sim 300$ kA, while the current direction gives $\kappa = -1$.

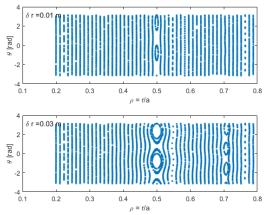

Figure 1: 2/1 islands for $\delta = 0.01$ and 0.03.

Poincaré sections of the magnetic field surfaces are shown in Fig. 1 for two perturbation amplitudes $\delta B/B_0 = 10^{-4}$ and $\delta B/B_0 = 10^{-3}$ corresponding to island sizes $\delta r = 0.01m, \delta r = 0.03m$, for the mode $(m,n) = (2,1)$ which is located at $r^*/a = 0.5$

III. Codes benchmarking. An ensemble of single particle trajectories is followed using both FO code (KORC [2]) and GC code (gcafpp). The background electron and ion temperatures are held fixed at $T_e = 1\,keV, T_i = 200\,eV$. Two benchmarking tests were run for FO and GC codes. First we started a distribution of Maxwellian particles at a single radius and followed it as function of time. The average radial spread gives the diffusion coefficient $D = \langle(\Delta r)^2\rangle/2t$. This should give neoclassical diffusion. Plotting D as function of density, which is related to collisionality (as seen in right panel), produces the diffusion regimes (banana, plateau, PS) which agree with neoclassical values as shown in Fig. 2(a) for FO with no islands present. In Fig. 2(b) D is plotted as function of the collision frequency for different island sizes when the initial radius is inside the island position ($\rho_0 = 0.3$) or outside ($\rho_0 = 0.7$). It is seen that the agreement with theory is good.

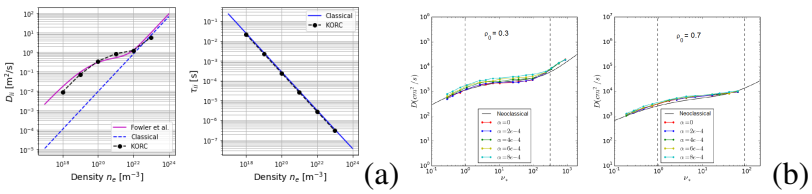

(a) (b)

Figure 2: Neoclassical diffusion for FO code and theory results (Fowler) (a) & GC for different island widths at 2 initial radii (b).

In the second benchmarking a fast ion population is evloved until thermalization is acheved for both codes. As shown in Fig. 3, the collisional thermalization times are of the same order ($t \approx 13\,ms$) in FO (a) and GC (b) simulations, for $n = 10^{20}m^{-3}, \mathscr{E} = 10$ keV. This gives confidence in codes comparison.

VI. Fast ion fluxes through islands. Initial ions have monoenergetic and mono-pitch-angle distributions on a single flux surface with $\rho < \rho^*$ and the number of particles N_{out} crossing a

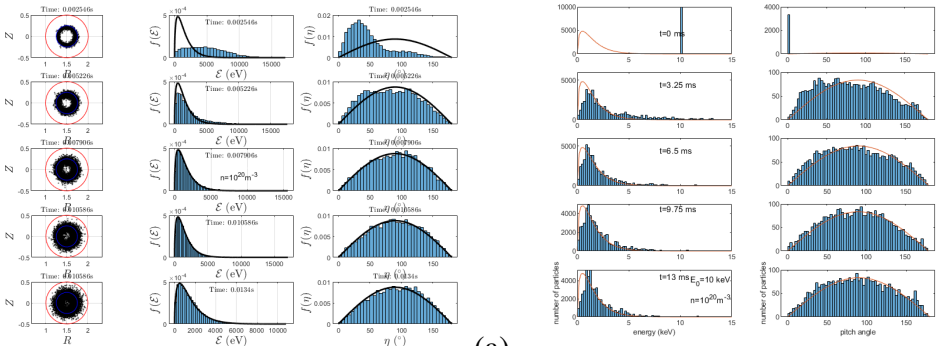

Figure 3: Distributions tend to Maxwellian in $\mathscr{E}$ and constant in pitch angle in same time for FO and GC codes.

surface at a radius $\rho = 0.54 > \rho^*$ is computed as function of time up to the slowing down time. We obtain a particle flux by fitting a quadratic to $N_{out}(t)$ and defining the flux as $\Gamma = dN_{out}/dt$. The flux rate of change is $d\Gamma/dt$.

In all simulations a $m/n = 2/1$ island is assumed in the rational surface where $q(r^*/a = 0.5) = 2$. The initial surface is at $\rho_{in} = r_{in}/a = 0.38 < \rho^*$. Simulations cover the parameter ranges: pitch angle $\eta = 0, 30^o$; $n = 10^{19} - 10^{20} m^{-3}$; $\mathscr{E} = 10$ keV -50 keV.

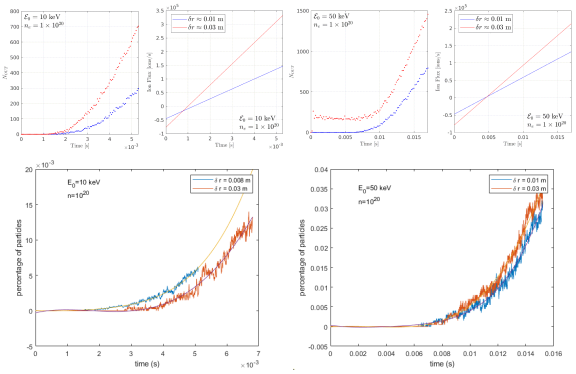

Figure 4: FO flows on top & GC flows (bottom) for mid-density & 2 island sizes ($\mathscr{E} = 10, 50$ keV).

In general, the particle flow increases as the island grows but the effect is less evident for higher densities. This effect is larger in the case of FO simulations than for the GC result as seen in Fig. 4, when N_{out} is computed for two different island sizes for $n = 10^{20} m^{-3}$ and two ion energies.

Fig. 5 shows the effect of changing density, energy and island size for two pitch angles using FO. The effect of η is to increase the flux since the FLR is larger but $d\Gamma/dt$ is reduced indicating steadier flux as FLR increases.

When island rotation is included $\omega \neq 0$ the FO flux increses much more than in GC. In FO, the co-rotation with J ($\omega > 0$) produce larger flux than counter-rotation $\omega < 0$, whereas in GC there is no difference. Focusing in the FO results, as the rotation frequency varies from 100 Hz to 100 kHz there is first an increase in particle flux and then a decrease

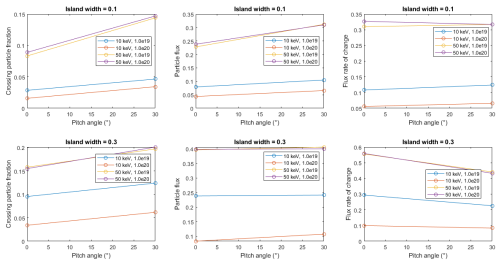

Figure 5: Flux dependence on pitch angle for FO varying $n, \mathscr{E}$ and δ.

with a maximum at $\omega \sim 10^4$ (see Fig. 6 for $\delta = 0.01$m; similar behavior is found for $\delta = 3$ cm). This indicates a resonant process.

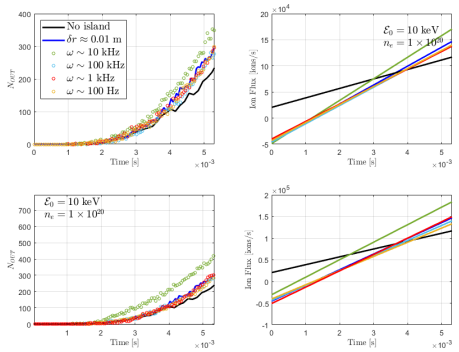

Figure 6: Ion fluxes for various rotations and narrow island.

The islands produced by NTM have an electric potential in and around the island with a 3D structure. While a poloidal flow driven by a radial E-field would reduce ion flux, in our case the ion flux is increased by the 3D electric field when there is no island rotation as sen in Fig. 7. Continuous lines are for no electric field, red is for wide island while blue is for narrow island.

V. Conclusions. The radial flux of fast ions across the rational surface containing magnetic islands is found to be modified in a variety of ways: (a) In FO and GC results, ions following the magnetic field lines cross the islands faster and thus wider islands produce larger fluxes than narrow islands. (b) Lower energy particles have a larger response to density changes that higher energies since they are less collisional. In turn larger n (more collisional) plasmas do not show a large increase of the radial flux since collisions deviate ions from magnetic island lines. (c) FLR effects increase island effectiveness to enhance ion flux. (d) A rotating island can produce increment ($\omega < 0$) or reduction ($\omega > 0$) of flux; this is a FO orbit effect since it is not present for GC simulations. (e) As function of ω flux first increases and then decreases indicating a resonant process with the rotation at $\omega \sim 10^4 Hz$. (f) The electric field associated with the island produces also an increase of the radial flux. This is a purely 3D effect of the E-field since a radial E-field reduces radial fluxes.

Acknowledgements. This work was partially supported by projects DGAPA-UNAM IN110021 and Conacyt A1-S-24157..

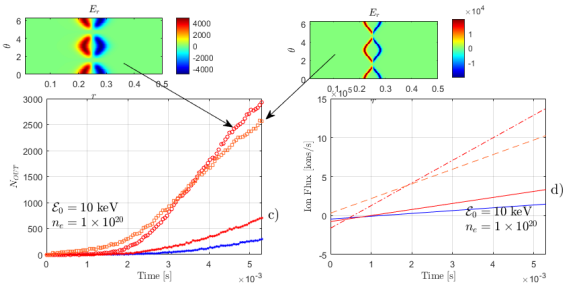

Figure 7: Electric field for two electric potentials produces larger ion flux.

[1] R.B. White, The theory of toroidally confined plasmas. World Scientific Publishing Company (2013).

[2] L. Carbajal, D. Del-Castillo-Negrete, D. Spong, S. Seal, L. Baylor, Phys. Plasmas, 24, 042512 (2017).

[3] L. Carbajal, D. del-Castillo-Negrete, J.J. Martinell, Physics of Plasmas 27, 032502 (2020).

[4] A. H. Boozer and G. Kuo-Petravic. Phys. Fluids, **24**, 851 (1981).